# Reliability Analysis of Subsea Pipelines under Spatially Varying Ground Motions by Using Subset Simulation

Yuyin Li[a], Yahui Zhang[a*], David Kennedy[b]

[a] *State Key Laboratory of Structural Analysis for Industrial Equipment, Department of Engineering Mechanics, International Center for Computational Mechanics, Dalian University of Technology, Dalian 116023, PR China;*

[b] *School of Engineering, Cardiff University, Cardiff CF24 3AA, Wales, UK*

Corresponding author:

Dr. Y. H. Zhang

State Key Laboratory of Structural Analysis for Industrial Equipment, Department of Engineering Mechanics, Dalian University of Technology, Dalian 116023, PR China

Email: zhangyh@dlut.edu.cn

Tel: +86 411 84706337

Fax: +86 411 84708393

# Abstract

A computational framework is presented to calculate the reliability of subsea pipelines subjected to a random earthquake. This framework takes full account of the physical features of pipelines and the earthquake, and also retains high computing precision and efficiency. The pipeline and the seabed are modelled as a Timoshenko beam and a Winkler foundation, respectively, while the unilateral contact effect between them is considered. The random earthquake is described by its power spectrum density function and its spatial variation is considered. After suitable discretizations in the spatial domain by the finite element method and the time domain by the Newmark integration method, the dynamic unilateral contact problem is derived as a linear complementarity problem (LCP). Subset Simulation (SS), which is an advanced Monte Carlo simulation approach, is used to estimate the reliability of pipelines. By means of numerical examples, the accuracy and robustness of SS are demonstrated by comparing with the direct Monte Carlo simulation (DMCS). Then a sensitivity analysis of the reliability and a failure analysis are performed to identify the influential system parameters. Finally, failure probabilities of subsea pipelines are assessed for three typical cases, namely, with and without the unilateral contact effect, with different grades of spatial variations and with different free spans. The influences of these effects or parameters on the reliability are discussed qualitatively.



**Key words**: subsea pipeline; random earthquake; spatially varying ground motion; unilateral contact; reliability; subset simulation

# 1 Introduction

Subsea pipelines always rest freely on the seabed, rather than being buried or anchored. Due to the scouring or unevenness of the seabed, pipelines will not touch down uniformly along the length of the pipe, and free spanning inevitably occurs. Since subsea pipelines are generally important and costly facilities, their reliability has been a fundamental problem of interest throughout the world. In recent years, attention has mainly been focused on corrosion failure [1], vortex-induced vibration fatigue damage [2], on-bottom lateral instability [3] and so on. As an occasional random excitation, a strong earthquake poses a tremendous threat to the safety of pipelines, and hence the dynamic response and reliability of pipelines under an earthquake have also received great attention. However, the emphasis has been on buried pipelines, with much less research on unburied pipelines. The relevant standards, such as DNV-OS-F101 [4], do not provide design methods or guidelines for the earthquake reliability of unburied subsea pipelines. The failure of structures under an earthquake is a typical first-excursion problem. To assess the first-excursion reliability, the main difficulties arise from (1) the solution of random responses of structures under the earthquake and (2) the evaluation of the reliability by using the random responses obtained in (1).

In the solution of random responses, one of the most important problems is how to consider the relationship between pipelines and seabed as exactly as possible. In the literature on the dynamic analysis of unburied pipelines, pipelines are widely simplified

60 as multi-supported beams or beams on an elastic foundation [5-8]. However, in reality
61 unburied pipelines are constrained unilaterally by the seabed, which means that the
62 reaction of the seabed can only be compressive, but not tensile. Hence, during the
63 vibration of pipelines, particularly when the deformation takes place predominantly in the
64 vertical plane, a separation of pipelines and the seabed will occur. Clearly, both the multi-
65 supported beam model and the elastic foundation beam model will overestimate the
66 constraint between pipelines and the seabed, and neither of these two models can take the
67 separation of pipelines and the seabed into consideration. Therefore, a unilateral contact
68 model is more appropriate to simulate the relationship between unburied pipelines and
69 the seabed, and such models have been applied to various kinds of static and dynamic
70 analysis of the subsea pipelines, such as the elastic and elasto-plastic analysis of subsea
71 pipelines subjected to vertical static loads [9], stress analysis problems involving subsea
72 pipelines freely resting upon irregular seabed profiles [10], optimal control of the dynamic
73 response of subsea cables constrained by a frictionless rigid seabed [11] and so on.
74 Nevertheless, due to the contact nonlinearity, obtaining the dynamic response of a
75 unilateral contact system is a challenging task, and some classical methods of structural
76 analysis, such as the analytical method used in [6] or the frequency-domain method used
77 in [8], are no longer feasible. As a consequence, the unilateral model is not used
78 frequently for the dynamic analysis of subsea pipelines under an earthquake, despite its
79 good approximation to the relationship between subsea pipelines and the seabed. In

general, the unilateral contact problem is dealt with by numerical methods, e.g., the combination of the finite element method and step-by-step integration method. In each time step, the nonlinear problem is solved by the Newton-Raphson method or a similar iterative method [10]. The unilateral contact problem can also be treated by deriving it as a linear complementary problem (LCP). There are many well-developed methods to solve the LCP and most of them have been included in commercial software, making it much more convenient to solve the unilateral contact method by the LCP method than Newton-Raphson methods.

The earthquake excitation model is another key point in the process of the solution of random responses of subsea pipelines. Due to the natural random factors of the soil, the motion of the seabed is more likely to exhibit strong randomness during an earthquake, as are the responses of structures. Hence it is more rational to study the responses of structures subjected to an earthquake from the point of view of the random vibration. On the other hand, variations can be found during earthquake wave propagation along the length of long-span structures, such as subsea pipelines, which result in differences in the amplitude and phase of ground motions at the supports of the structures. This phenomenon is termed as spatially varying ground motions [13]. Many random vibration methods have been developed for the analysis of multi-span structures subjected to spatially varying ground motions [14-16]. However, these methods are no longer feasible after taking the contact of pipelines and the seabed into consideration, for two reasons.

100 Firstly, these methods are based on the power spectrum density or response spectrum,
101 which are essentially frequency-domain methods, and thus cannot be used to treat the
102 contact problem because of the nonlinearity. Secondly, the response of a nonlinear system
103 is always non-Gaussian even if the input is a Gaussian random process, and these methods
104 can only provide the first- and second-order statistical moments of the response, which
105 are insufficient to describe totally the statistical properties of the non-Gaussian response.
106 In the circumstances, the Monte Carlo simulation (MCS) method, which is suitable for
107 both linear and nonlinear random vibration analysis, seems to be the best and only choice,
108 despite its relatively large computational requirements [17].

109 After obtaining the random response of subsea pipelines, the problem which follows
110 is how to estimate the reliability of subsea pipelines through this random response. Due
111 to the complex nature of the first-excursion failure and the unilateral contact problem, the
112 limit state function of subsea pipelines is extremely complicated and has no explicit
113 expression, while extreme values of the random response are not Gaussian distributed.
114 Therefore, popular methods of reliability analysis such as the first order reliability method
115 (FORM) [18], second order reliability method (SORM) [19], point estimate method
116 (PEM) [20], etc. are unable to predict accurately the reliability of subsea pipelines under
117 an earthquake. The MCS is one of most well-known methods for reliability analysis
118 because it is independent of the complexity and dimension of the problem. However, the
119 number of samples required by the MCS is proportional to the reciprocal of the failure

120 probability. Hence, when the failure probability is very small, e.g., of order $10^{-3}$, this
121 method will suffer from inefficiency due to its demand for a large number of samples. In
122 order to reduce the computational cost of the MCS, an advanced MCS called Importance
123 Sampling (IS) was developed [21,22]. The IS requires prior knowledge of the system in
124 the failure region, so it works well when applied to a linear and low-dimensional problem,
125 whose failure region is quite simple. However, the failure region geometry of subsea
126 pipelines under an earthquake is complicated and prior knowledge of the random
127 responses is unavailable, hence the IS is not suitable for the problem considered in this
128 paper. In order to carry out reliability analysis with small failure probabilities, Au et al.
129 [23,24] developed another advanced MCS named Subset Simulation (SS). The basic idea
130 of SS is to express a small failure probability event as a product of a series of intermediate
131 events with larger conditional probabilities. Through setting these intermediate events
132 properly, the conditional probabilities can be large enough to be estimated with a small
133 number of samples. SS is a robust and efficient method and has been used for predicting
134 small failure probabilities in engineering fields, such as the time-dependent reliability of
135 underground flexible pipelines [25], the probabilistic dynamic behaviour of mistuned
136 bladed disc systems [26], radioactive waste repository performance assessment [27], the
137 stochastic dynamic stiffness of foundations for large offshore wind turbines [28] and so
138 on. A general form of SS is presented in [29] is mainly, with application to a seismic risk
139 problem involving dynamic analysis.

As mentioned above, reliability analysis of subsea pipelines subjected to random earthquakes faces two difficulties: the solution of random responses and estimation of reliability, and these are the focus of this paper. Regarding random response solutions, mathematical models with reasonable simplifications and assumptions are firstly estimated for pipelines, seabed and ground motions, and then a corresponding solution strategy is given based on LCP. Regarding reliability estimation, SS is introduced to increase the computational efficiency for the predictions of first-excursion failure probabilities of pipelines. This paper therefore provides a practical computational framework for the reliability analysis of subsea pipelines subjected to random earthquakes. The work is structured as follows. In section 2, the mathematical formulation of a subsea pipeline under a random earthquake is given. In section 3, by combining the finite element method and Newmark integration method, a solution strategy is obtained by deriving the unilateral contact problem as a LCP. In section 4 the fundamental concept and implementation procedures of SS are briefly presented. Section 5 gives some numerical examples. The feasibility of SS is verified with respect to direct MCS, and the contribution of some random parameters to the failure of pipelines is addressed through a sensitivity analysis. Then, influences of the unilateral contact effect, the spatial variation and the free span on the reliability of pipelines are investigated. Finally, conclusions are given in section 6.

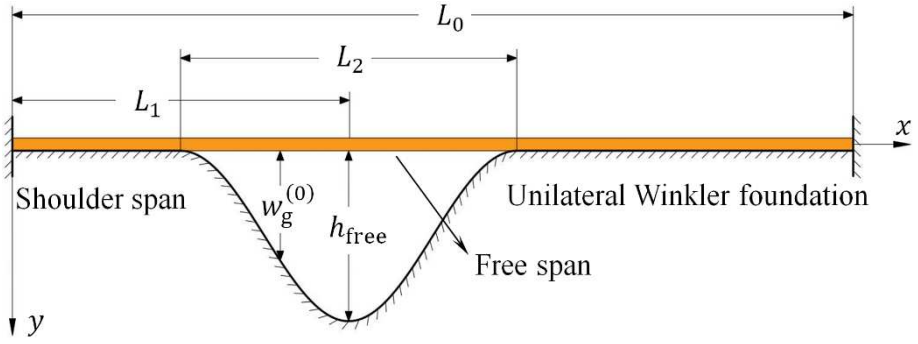


(a) Without deformation

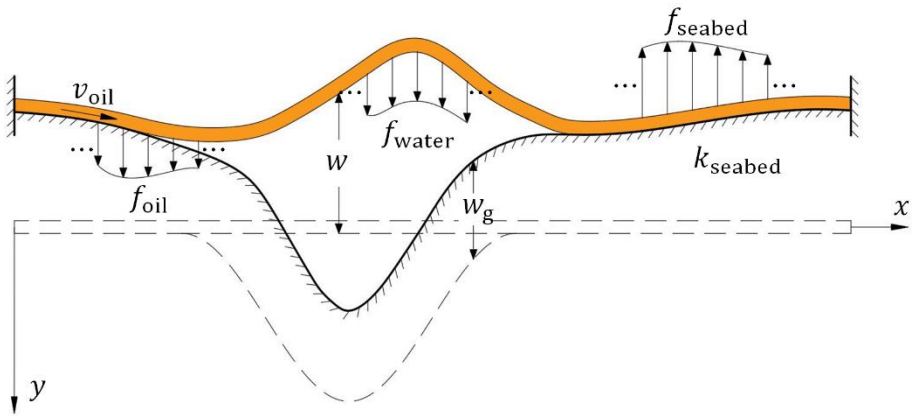


(b) With deformation

**Fig. 1.** Schematic of a subsea pipeline

# 2 Problem formulations

## 2.1 Governing equations of the pipeline

A schematic of a subsea pipeline and the seabed is shown in Fig. 1(a). There is a free span in the middle of the pipeline due to the scouring or unevenness of the seabed. The length of the pipeline is denoted by $L_0$, while the location and length of the free span are denoted by $L_1$ and $L_2$, respectively. Because of the complex formation mechanism and

173 the lack of practical measured data of the free span, the seabed profile $w_{\mathrm{g}}^{(0)}$ is

174 approximated with the following function

175

$$w_{\mathrm{g}}^{(0)} = \begin{cases} 0 & 0 \le x < L_1 - L_2/2 \\ \dfrac{h_{\mathrm{free}}}{2}\left[1 - \cos\dfrac{2\pi(x - L_1 + L_2/2)}{L_2}\right] & L_1 - L_2/2 \le x < L_1 + L_2/2 \\ 0 & L_1 + L_2/2 \le x \le L_0 \end{cases} \quad (1)$$

176

177 where $h_{\mathrm{free}}$ is the maximum depth of the free span.

178 The pipeline is modelled based on the Timoshenko beam theory and hydrodynamic

179 forces of the internal oil and the surrounding seawater are considered. The seabed is

180 simplified as a Winkler foundation. In the coordinates shown in Fig. 1(b), the governing

181 equations for the vibration of the pipeline in the vertical plane can be written as

182

$$\begin{aligned} &\rho I\frac{\partial^2\theta}{\partial t^2} - EI\frac{\partial^2\theta}{\partial x^2} - \kappa GA\left(\frac{\partial w}{\partial x} - \theta\right) + d_1\rho I\frac{\partial\theta}{\partial t} \\ &\qquad - d_2\left[EI\frac{\partial^3\theta}{\partial x^2\partial t} + \kappa GA\left(\frac{\partial^2 w}{\partial x\partial t} - \frac{\partial\theta}{\partial t}\right)\right] = M_{\mathrm{oil}} \\ &m_{\mathrm{pipe}}\frac{\partial^2 w}{\partial t^2} - \kappa GA\left(\frac{\partial^2 w}{\partial x^2} - \frac{\partial\theta}{\partial x}\right) + d_1 m_{\mathrm{pipe}}\frac{\partial w}{\partial t} - d_2\kappa GA\left(\frac{\partial^3 w}{\partial x^2\partial t} - \frac{\partial^2\theta}{\partial x\partial t}\right) \\ &\qquad + N_0\frac{\partial^2 w}{\partial x^2} = f_{\mathrm{oil}} + f_{\mathrm{water}} - f_{\mathrm{seabed}} \end{aligned} \quad (2)$$

183

184 where $t$ is time, $\theta$ is the cross-section rotation, $w$ is the vertical displacement of the

185 pipeline, $\rho I$ is the moment of inertia, $EI$ is the flexural rigidity, $\kappa GA$ is the effective

186 shear rigidity, $m_{\mathrm{pipe}}$ is the mass per unit length, $d_1$ and $d_2$ are Rayleigh damping

187 factors corresponding to the mass and stiffness, respectively, $N_0$ is the axial compression,

188 $M_{\mathrm{oil}}$ and $f_{\mathrm{oil}}$ are respectively the hydrodynamic forces per unit length in the rotational

and vertical directions, $f_{\mathrm{water}}$ is the hydrodynamic force per unit length due to the surrounding seawater, and $f_{\mathrm{seabed}}$ is the reaction force per unit length of the seabed.

It is assumed that the internal oil is an incompressible and inviscid fluid with a constant flow velocity $v_{\mathrm{oil}}$, and the effects of the oil are considered as external forces on the pipeline. Thus, as a fluid-conveying beam [30], $M_{\mathrm{oil}}$ and $f_{\mathrm{oil}}$ can be expressed as

$$\begin{aligned} M_{\mathrm{oil}} &= -\rho_{\mathrm{oil}} I_{\mathrm{oil}} \frac{\partial^2 \theta}{\partial x^2} \\ f_{\mathrm{oil}} &= -m_{\mathrm{oil}} v_{\mathrm{oil}}^2 \frac{\partial^2 w}{\partial x^2} - 2 m_{\mathrm{oil}} v_{\mathrm{oil}} \frac{\partial^2 w}{\partial x \partial t} - m_{\mathrm{oil}} \frac{\partial^2 w}{\partial t^2} \end{aligned} \tag{3}$$

in which $\rho_{\mathrm{oil}} I_{\mathrm{oil}}$ is the moment of inertia of the oil and $m_{\mathrm{oil}}$ is its mass per unit length.

For slender cylindrical structures such as pipelines, Morison's equation [31] is widely used to evaluate the resulting hydrodynamic force of the surrounding water, defined as the summation of the inertia and drag forces. It is assumed that the surrounding water is static, while the drag force is small and hence can be neglected, so that $f_{\mathrm{water}}$ is determined by

$$f_{\mathrm{water}} = -C_{\mathrm{m}} \rho_{\mathrm{water}} \pi R_{\mathrm{out}}^2 \frac{\partial^2 w}{\partial t^2} \tag{4}$$

where $C_{\mathrm{m}}$ is the added mass coefficient and is generally equal to 1.0, $\rho_{\mathrm{water}}$ is the density of the seawater and $R_{\mathrm{out}}$ is the outer radius of the pipe.

The friction of the seabed is ignored. Unilateral contact in the vertical plane is considered, and thus the reaction force of the seabed $f_{\mathrm{seabed}}$ is

$$f_{\text{seabed}} = \begin{cases} 0 & \xi > 0 \\ \lambda k_{\text{seabed}} & \xi = 0 \end{cases} \tag{5}$$

where $k_{\text{seabed}}$ is the stiffness of the seabed, and

$$\xi = \lambda + w_{\text{g}}^{(0)} + w_{\text{g}} - w \tag{6}$$

is the relative displacement between the pipe and the seabed, $\lambda$ is the compressional deformation of the seabed, $w_{\text{g}}^{(0)}$ is the initial profile of the seabed and $w_{\text{g}}$ is the motion of the seabed. Since the pipeline is constrained unilaterally by the seabed, the reaction of the seabed can only be compressive, but not tensile. On the other hand, the pipe can be either above or in contact with the seabed, but never under it. Hence, $f_{\text{seabed}}$ and $\xi$ satisfy the following linear complementarity conditions,

$$\xi \geq 0, \qquad f_{\text{seabed}} \geq 0, \qquad \xi f_{\text{seabed}} = 0 \tag{7}$$

Obtaining the solution of Eq. (2) is a quite challenging task because of two difficulties. Firstly, the earthquake is a random process and the spatial variation is considered, so the motion of the seabed is actually a random field. Secondly, contact regions of the pipeline and seabed are not known a priori and will change with the pipeline motion. The contact nonlinearity further increases the difficulty of solution.

## 2.2 Random earthquake with spatial variation

The acceleration of the ground motion due to the earthquake is assumed to be a nonstationary random process which can be expressed as

$$\ddot{w}_{\mathrm{g}} = g(t)\ddot{d}(t) \tag{8}$$

where $\ddot{d}(t)$ is a stationary Gaussian random process with zero mean value and $g(t)$ is a slowly varying deterministic envelope function which is given as

$$g(t) = 2.5974(\mathrm{e}^{-0.2t} - \mathrm{e}^{-0.6t}) \tag{9}$$

Assuming that $\ddot{d}(t)$ is homogeneous in the spatial domain, then the cross power spectral density (PSD) of the acceleration at two arbitrary points can be expressed as

$$S\,(\Delta x, \omega) = \gamma(\Delta x, \omega) S_0(\omega) \tag{10}$$

where $\omega$ is the circular frequency, $\Delta x = \left|x_i - x_j\right|$ is the distance between the two points $x_i$ and $x_j$ on the ground, $S_0(\omega)$ is the auto-PSD of the acceleration of the ground motion and $\gamma(\Delta x, \omega)$ is the coherency function which can be written as

$$\gamma(\Delta x, \omega) = \gamma^{(\mathrm{w})}(\Delta x, \omega)\gamma^{(\mathrm{c})}(\Delta x, \omega) \tag{11}$$

in which

$$\gamma^{(\mathrm{w})}(\Delta x, \omega) = \exp\left(-\frac{\mathrm{i}\omega\Delta x}{v_{\mathrm{app}}}\right) \tag{12}$$

indicates the complex-valued wave passage effect, $\mathrm{i} = \sqrt{-1}$, $v_{\mathrm{app}}$ is the apparent velocity of the earthquake waves, and

$$\gamma^{(c)}(\Delta x, \omega) = \exp\left(-\alpha \frac{\omega \Delta x}{2\pi v_{\text{app}}}\right) \tag{13}$$

characterizes the real-valued incoherence effect. The L-Y model [32] is used in this paper and $\alpha = 0.125$. The modified Kanai-Tajimi PSD of the acceleration is used and $S_0$ is given by [33]

$$S_0(\omega) = \frac{1 + 4\xi_{\text{g}}^2\left(\omega/\omega_{\text{g}}\right)^2}{\left[1 - \left(\omega/\omega_{\text{g}}\right)^2\right]^2 + 4\xi_{\text{g}}^2\left(\omega/\omega_{\text{g}}\right)^2} \times \frac{(\omega/\omega_{\text{f}})^4}{[1 - (\omega/\omega_{\text{f}})^2]^2 + 4\xi_{\text{f}}^2(\omega/\omega_{\text{f}})^2} S_{\text{g}} \tag{14}$$

where $\omega_{\text{g}}$ and $\xi_{\text{g}}$ are the resonant frequency and damping ratio of the first filter, and $\omega_{\text{f}}$ and $\xi_{\text{f}}$ are those of the second filter. $S_{\text{g}}$ is the amplitude of the white-noise bedrock acceleration which depends on the soil condition.

Since the SS used in this paper is based on the MCS method, the time history samples of the ground motion should be generated from the PSD of the acceleration as shown in Eq. (10). Here the Auto-Regressive Moving-Average (ARMA) method is used to generate the time history samples of the ground acceleration. For brevity in this paper, details of the ARMA are not presented and interested readers are referred to [34]. In addition, since it is required to estimate the force acting on the pipeline, and to detect the contact between the pipeline and the seabed in each time step, the time histories of the velocity and displacement of the seabed also need to be evaluated. A simple and direct approach to

obtaining the velocity and displacement is to make use of the inherent integral relations between the displacement, velocity and acceleration by assuming zero initial conditions. However, due to the accumulation of random noise in accelerations, direct integration of the acceleration data often causes unrealistic drifts, namely baseline offsets in the velocity and displacement. In order to eliminate the baseline offsets, a commonly used correction scheme suggested by Berg and Housner [35] is used, in which the zero-acceleration baseline is assumed to be of polynomial form, the constants of which are determined by minimizing the mean square computed velocity.

# 3 Linear complementarity method for the dynamic contact of pipeline and seabed

Because of the contact nonlinearity, it is impossible to obtain an analytical solution of Eq. (2). Numerical solution seems to be the only choice, and thus a suitable discretization is needed in the spatial and time domains. The pipeline is discretized into Timoshenko beam elements with two nodes, considering the effects of both the oil conveyed through the pipeline and the surrounding seawater, while the seabed is modelled as spring elements. Considering the spatial variation of the ground motion, the governing equation of the pipeline can be represented in the following discrete form,

$$\begin{bmatrix} \boldsymbol{M}_{\mathrm{s}} & \boldsymbol{M}_{\mathrm{sb}} \\ \boldsymbol{M}_{\mathrm{sb}}^{\mathrm{T}} & \boldsymbol{M}_{\mathrm{b}} \end{bmatrix} \begin{Bmatrix} \ddot{\boldsymbol{X}}_{\mathrm{s}} \\ \ddot{\boldsymbol{X}}_{\mathrm{b}} \end{Bmatrix} + \begin{bmatrix} \boldsymbol{C}_{\mathrm{s}} & \boldsymbol{C}_{\mathrm{sb}} \\ \boldsymbol{C}_{\mathrm{sb}}^{T} & \boldsymbol{C}_{\mathrm{b}} \end{bmatrix} \begin{Bmatrix} \dot{\boldsymbol{X}}_{\mathrm{s}} \\ \dot{\boldsymbol{X}}_{\mathrm{b}} \end{Bmatrix} + \begin{bmatrix} \boldsymbol{K}_{\mathrm{s}} & \boldsymbol{K}_{\mathrm{sb}} \\ \boldsymbol{K}_{\mathrm{sb}}^{\mathrm{T}} & \boldsymbol{K}_{\mathrm{b}} \end{bmatrix} \begin{Bmatrix} \boldsymbol{X}_{\mathrm{s}} \\ \boldsymbol{X}_{\mathrm{b}} \end{Bmatrix} = \begin{Bmatrix} \boldsymbol{R}_{\mathrm{s}} \\ \boldsymbol{R}_{\mathrm{b}} \end{Bmatrix} \tag{15}$$

in which the subscripts "b" and "s" indicate the support and non-support degrees of freedom (DOF), respectively, so that $\boldsymbol{X}_\mathrm{b}$ are the enforced displacements of the supports on both sides, $\boldsymbol{X}_\mathrm{s}$ are all nodal displacements except those at the supports, $\boldsymbol{R}_\mathrm{b}$ are the enforced forces at the supports and $\boldsymbol{R}_\mathrm{s}$ are the reaction forces of the seabed. $\boldsymbol{M}$, $\boldsymbol{C}$ and $\boldsymbol{K}$ are the mass, damping and stiffness matrices, respectively. Expanding the first row of Eq. (15) gives

$$\boldsymbol{M}_\mathrm{s}\ddot{\boldsymbol{X}}_\mathrm{s} + \boldsymbol{C}_\mathrm{s}\dot{\boldsymbol{X}}_\mathrm{s} + \boldsymbol{K}_\mathrm{s}\boldsymbol{X}_\mathrm{s} = \boldsymbol{R}_\mathrm{s} + \boldsymbol{P} \tag{16}$$

where $\boldsymbol{P} = -\boldsymbol{M}_\mathrm{sb}\ddot{\boldsymbol{X}}_\mathrm{b} - \boldsymbol{C}_\mathrm{sb}\dot{\boldsymbol{X}}_\mathrm{b} - \boldsymbol{K}_\mathrm{sb}\boldsymbol{X}_\mathrm{b}$ is the effective earthquake force acting on the non-support DOF.

Each node of the beam element used in this paper has two DOF, namely translation and rotation in the vertical plane. However, it is assumed that the reaction force of the seabed acts only on the translation DOF. For the convenience of the following derivation procedures, rearranging the DOF in Eq. (16) gives

$$\begin{bmatrix} \boldsymbol{M}_\mathrm{w} & \boldsymbol{M}_\mathrm{wq} \\ \boldsymbol{M}_\mathrm{qw} & \boldsymbol{M}_\mathrm{q} \end{bmatrix} \begin{Bmatrix} \ddot{\boldsymbol{w}} \\ \ddot{\boldsymbol{q}} \end{Bmatrix} + \begin{bmatrix} \boldsymbol{C}_\mathrm{w} & \boldsymbol{C}_\mathrm{wq} \\ \boldsymbol{C}_\mathrm{qw} & \boldsymbol{C}_\mathrm{q} \end{bmatrix} \begin{Bmatrix} \dot{\boldsymbol{w}} \\ \dot{\boldsymbol{q}} \end{Bmatrix} + \begin{bmatrix} \boldsymbol{K}_\mathrm{w} & \boldsymbol{K}_\mathrm{wq} \\ \boldsymbol{K}_\mathrm{qw} & \boldsymbol{K}_\mathrm{q} \end{bmatrix} \begin{Bmatrix} \boldsymbol{w} \\ \boldsymbol{q} \end{Bmatrix} = \begin{Bmatrix} \boldsymbol{r}_\mathrm{w} \\ \boldsymbol{0} \end{Bmatrix} + \begin{Bmatrix} \boldsymbol{P}_\mathrm{w} \\ \boldsymbol{P}_\mathrm{q} \end{Bmatrix} \tag{17}$$

where $\boldsymbol{w}$ and $\boldsymbol{q}$ are the translation and rotation DOF, respectively; $\boldsymbol{P}_\mathrm{w}$ and $\boldsymbol{P}_\mathrm{q}$ are the effective forces acting on the translation and rotation DOF, respectively, and $\boldsymbol{r}_\mathrm{w}$ is the reaction force of the seabed.

306 Based on the Newmark integration method, Eq. (17) is discretized in the time domain.

307 With appropriate gathering of terms, the governing equation at time $t_{k+1}$ can be written

308 as

309

$$\begin{bmatrix} \widehat{\boldsymbol{K}}_{\mathrm{w}} & \widehat{\boldsymbol{K}}_{\mathrm{wq}} \\ \widehat{\boldsymbol{K}}_{\mathrm{qw}} & \widehat{\boldsymbol{K}}_{\mathrm{q}} \end{bmatrix} \begin{Bmatrix} \boldsymbol{w} \\ \boldsymbol{q} \end{Bmatrix}_{k+1} = \begin{Bmatrix} \boldsymbol{r}_{\mathrm{w}} \\ \boldsymbol{0} \end{Bmatrix}_{k+1} + \begin{Bmatrix} \widehat{\boldsymbol{P}}_{\mathrm{w}} \\ \widehat{\boldsymbol{P}}_{\mathrm{q}} \end{Bmatrix}_{k+1} \tag{18}$$

310

311 where

312

$$\begin{bmatrix} \widehat{\boldsymbol{K}}_{\mathrm{w}} & \widehat{\boldsymbol{K}}_{\mathrm{wq}} \\ \widehat{\boldsymbol{K}}_{\mathrm{qw}} & \widehat{\boldsymbol{K}}_{\mathrm{q}} \end{bmatrix} = \begin{bmatrix} \boldsymbol{K}_{\mathrm{w}} & \boldsymbol{K}_{\mathrm{wq}} \\ \boldsymbol{K}_{\mathrm{qw}} & \boldsymbol{K}_{\mathrm{q}} \end{bmatrix} + a_0 \begin{bmatrix} \boldsymbol{M}_{\mathrm{w}} & \boldsymbol{M}_{\mathrm{wq}} \\ \boldsymbol{M}_{\mathrm{qw}} & \boldsymbol{M}_{\mathrm{q}} \end{bmatrix} + a_1 \begin{bmatrix} \boldsymbol{C}_{\mathrm{w}} & \boldsymbol{C}_{\mathrm{wq}} \\ \boldsymbol{C}_{\mathrm{qw}} & \boldsymbol{C}_{\mathrm{q}} \end{bmatrix} \tag{19}$$

313

$$\begin{aligned} \begin{Bmatrix} \widehat{\boldsymbol{P}}_{\mathrm{w}} \\ \widehat{\boldsymbol{P}}_{\mathrm{q}} \end{Bmatrix}_{k+1} = \begin{Bmatrix} \boldsymbol{P}_{\mathrm{w}} \\ \boldsymbol{P}_{\mathrm{q}} \end{Bmatrix}_{k+1} &+ \begin{bmatrix} \boldsymbol{M}_{\mathrm{w}} & \boldsymbol{M}_{\mathrm{wq}} \\ \boldsymbol{M}_{\mathrm{qw}} & \boldsymbol{M}_{\mathrm{q}} \end{bmatrix} \left( a_0 \begin{Bmatrix} \boldsymbol{w} \\ \boldsymbol{q} \end{Bmatrix}_k + a_2 \begin{Bmatrix} \dot{\boldsymbol{w}} \\ \dot{\boldsymbol{q}} \end{Bmatrix}_k + a_3 \begin{Bmatrix} \ddot{\boldsymbol{w}} \\ \ddot{\boldsymbol{q}} \end{Bmatrix}_k \right) \\ &+ \begin{bmatrix} \boldsymbol{C}_{\mathrm{w}} & \boldsymbol{C}_{\mathrm{wq}} \\ \boldsymbol{C}_{\mathrm{qw}} & \boldsymbol{C}_{\mathrm{q}} \end{bmatrix} \left( a_1 \begin{Bmatrix} \boldsymbol{w} \\ \boldsymbol{q} \end{Bmatrix}_k + a_4 \begin{Bmatrix} \dot{\boldsymbol{w}} \\ \dot{\boldsymbol{q}} \end{Bmatrix}_k + a_5 \begin{Bmatrix} \ddot{\boldsymbol{w}} \\ \ddot{\boldsymbol{q}} \end{Bmatrix}_k \right) \end{aligned} \tag{20}$$

314

$$\begin{aligned} a_0 = \frac{1}{\alpha(\Delta t)^2} \quad a_1 = \frac{\delta}{\alpha \Delta t} \quad a_2 = \frac{1}{\alpha \Delta t} \quad a_3 = \frac{1}{2\alpha} - 1 \\ a_4 = \frac{\delta}{\alpha} - 1 \quad a_5 = \frac{\Delta t}{2}\left(\frac{\delta}{\alpha} - 2\right) \end{aligned} \tag{21}$$

315

316 in which $\Delta t$ is the time step, $\delta$ and $\alpha$ are parameters of the Newmark integration

317 method, which satisfy $\delta \geq 0.5$ and $\alpha \geq 0.25(0.5+\delta)^2$ to ensure the unconditional

318 stability of the integration scheme. The acceleration and the velocity at time $t_{k+1}$ are

319

$$\begin{aligned} \begin{Bmatrix} \ddot{\boldsymbol{w}} \\ \ddot{\boldsymbol{q}} \end{Bmatrix}_{k+1} &= a_0 \left( \begin{Bmatrix} \boldsymbol{w} \\ \boldsymbol{q} \end{Bmatrix}_{k+1} - \begin{Bmatrix} \boldsymbol{w} \\ \boldsymbol{q} \end{Bmatrix}_k \right) - a_2 \begin{Bmatrix} \dot{\boldsymbol{w}} \\ \dot{\boldsymbol{q}} \end{Bmatrix}_k - a_3 \begin{Bmatrix} \ddot{\boldsymbol{w}} \\ \ddot{\boldsymbol{q}} \end{Bmatrix}_k \\ \begin{Bmatrix} \dot{\boldsymbol{w}} \\ \dot{\boldsymbol{q}} \end{Bmatrix}_{k+1} &= \begin{Bmatrix} \dot{\boldsymbol{w}} \\ \dot{\boldsymbol{q}} \end{Bmatrix}_k + a_6 \begin{Bmatrix} \ddot{\boldsymbol{w}} \\ \ddot{\boldsymbol{q}} \end{Bmatrix}_k + a_7 \begin{Bmatrix} \ddot{\boldsymbol{w}} \\ \ddot{\boldsymbol{q}} \end{Bmatrix}_{k+1} \end{aligned} \tag{22}$$

320

in which $a_6 = \Delta t(1-\delta)$ and $a_7 = \delta\Delta t$.

Expanding Eq. (18) and eliminating terms related to $\boldsymbol{q}$ gives

$$\overline{\boldsymbol{K}}_{\mathrm{w}}\boldsymbol{w}_{k+1} = \boldsymbol{r}_{\mathrm{w},k+1} + \overline{\boldsymbol{P}}_{\mathrm{w},k+1} \tag{23}$$

where $\overline{\boldsymbol{K}}_{\mathrm{w}} = \widehat{\boldsymbol{K}}_{\mathrm{w}} - \widehat{\boldsymbol{K}}_{\mathrm{wq}}\widehat{\boldsymbol{K}}_{\mathrm{q}}^{-1}\widehat{\boldsymbol{K}}_{\mathrm{qw}}$ and $\overline{\boldsymbol{P}}_{\mathrm{w},k+1} = \widehat{\boldsymbol{P}}_{\mathrm{w},k+1} - \widehat{\boldsymbol{K}}_{\mathrm{wq}}\widehat{\boldsymbol{K}}_{\mathrm{q}}^{-1}\widehat{\boldsymbol{P}}_{\mathrm{q},k+1}$.

According to Eq. (6), the relative vertical distance between the seabed and pipeline at time $t_{k+1}$ is

$$\boldsymbol{\xi}_{k+1} = \boldsymbol{\lambda}_{k+1} + \boldsymbol{w}_{\mathrm{g}}^{(0)} + \boldsymbol{w}_{\mathrm{g},k+1} - \boldsymbol{w}_{k+1} \tag{24}$$

where

$$\boldsymbol{\lambda}_{k+1} = \boldsymbol{K}_{\mathrm{g}}^{-1}\boldsymbol{r}_{\mathrm{w},k+1} \tag{25}$$

is the compressional deformation of the seabed at time $t_{k+1}$, $\boldsymbol{K}_{\mathrm{g}}$ is the stiffness matrix of the seabed and $\boldsymbol{w}_{\mathrm{g}}^{(0)}$ is the initial profile of the seabed.

Combining Eqs. (23) to (25) gives

$$\widetilde{\boldsymbol{K}}\boldsymbol{\xi}_{k+1} = \boldsymbol{r}_{\mathrm{w},k+1} + \widetilde{\boldsymbol{P}}_{\mathrm{w},k+1} \tag{26}$$

in which $\widetilde{\boldsymbol{K}} = \left(\overline{\boldsymbol{K}}_{\mathrm{w}}\boldsymbol{K}_{\mathrm{g}}^{-1} - \boldsymbol{I}\right)^{-1}\overline{\boldsymbol{K}}_{\mathrm{w}}$, $\widetilde{\boldsymbol{P}}_{\mathrm{w},k+1} = \left(\overline{\boldsymbol{K}}_{\mathrm{w}}\boldsymbol{K}_{\mathrm{g}}^{-1} - \boldsymbol{I}\right)^{-1}\left[\overline{\boldsymbol{K}}_{\mathrm{w}}\left(\boldsymbol{w}_{\mathrm{g}}^{(0)} + \boldsymbol{w}_{\mathrm{g},k+1}\right) - \overline{\boldsymbol{P}}_{\mathrm{w},k+1}\right]$ and $\boldsymbol{I}$ is an identity matrix.

Eq. (7) can be expressed in the following discretized form

$$\boldsymbol{\xi}_{k+1} \geq \mathbf{0}, \qquad \boldsymbol{r}_{\mathrm{w},k+1} \geq \mathbf{0}, \qquad \boldsymbol{\xi}_{k+1}^{\mathrm{T}} \boldsymbol{r}_{\mathrm{w},k+1} = 0 \tag{27}$$

Eqs. (26) and (27) together form a mathematical structure known as a LCP, which is equivalent to the following quadratic programming problem

$$\begin{aligned} \min f(\boldsymbol{\xi}_{k+1}) &= \frac{1}{2} \boldsymbol{\xi}_{k+1}^{\mathrm{T}} \widetilde{\boldsymbol{K}} \boldsymbol{\xi}_{k+1} - \widetilde{\boldsymbol{P}}_{\mathrm{w},k+1}^{\mathrm{T}} \boldsymbol{\xi}_{k+1} \\ \text{s.t. } & \boldsymbol{\xi}_{k+1} \geq \mathbf{0} \end{aligned} \tag{28}$$

Because of the symmetry and positive definiteness of $\widetilde{\boldsymbol{K}}$, Eq. (28) is a convex optimization problem and the common solution to it is guaranteed to exist and be unique [12]. There are many well-developed methods to solve the LCP and most of them have been included in some commercial software. For simplicity, the solution procedures of the LCP are not given in this paper.

By solving the LCP problem of Eq. (28), $\boldsymbol{\xi}_{k+1}$ can be determined. Then, by substituting $\boldsymbol{\xi}_{k+1}$ into Eq. (26), the reaction force of the seabed $\boldsymbol{r}_{\mathrm{w},k+1}$ is obtained. The displacement of the pipeline $\boldsymbol{w}_{k+1}$ is further determined by substituting $\boldsymbol{r}_{\mathrm{w},k+1}$ into Eq. (23). It is worthwhile to point out that an iterative procedure is needed in most solution methods for the LCP, and thus the solution at the current time step can be used as the initial trial solution for the next time step in order to accelerate convergence.

# 4 Subset simulation for reliability estimation

The first-excursion probabilities of a subsea pipeline subjected to a spatially varying

ground motion are considered in this paper. The failure event of the pipelines can be represented as the exceedance of an arbitrary response $\boldsymbol{s}(t,\boldsymbol{\theta})$, which can be the displacement, internal force, stress or any other response, above the threshold value $b$ within a specified time interval, i.e.,

$$F = \left\{ \max_{l=1,\cdots,n_r} \left( \max_{t\in[0,T]} |\boldsymbol{s}(t,\boldsymbol{\theta})| \right) > b \right\} \tag{29}$$

where $n_r$ denotes the dimension of the response $\boldsymbol{s}(t,\boldsymbol{\theta})$, $T$ is the duration of the earthquake, $\boldsymbol{\theta}$ is a random variable vector which characterizes the randomness in the system, and whose probability density function (PDF) is $q(\boldsymbol{\theta})$. It is noted that bending stresses are used to identify the failure of pipelines in this paper. The probability of the occurrence of the failure event $F$, namely, the failure probability, can be expressed in terms of the following probability integral

$$P(F) = \int_{\boldsymbol{\theta}\in\boldsymbol{\Omega}} I_F(\boldsymbol{\theta}) q(\boldsymbol{\theta})\, \mathrm{d}\boldsymbol{\theta} \tag{30}$$

where $I_F$ is the indicator function, which is equal to 1 when the pipeline has failed and 0 otherwise. $\boldsymbol{\Omega}$ denotes the value space of $\boldsymbol{\theta}$.

Generally, the integral in Eq. (30) cannot be calculated efficiently by means of direct numerical integration due to the high dimension of $\boldsymbol{\theta}$ and the complicated geometry of the failure region. MCS is commonly used in problems with high dimension and a complicated failure region, by virtue of its computational robustness. However, the main

drawback of MCS is that it is not suitable for evaluating small failure probabilities due to its demand for a large number of samples. In order to reduce the computational cost of MCS, SS [23, 24] is used, of which the main procedures are as follows.

By introducing a sequence of ascending threshold values $0 < b_1 < b_2 < \cdots < b_n = b$, one can obtain the corresponding intermediate failure events $F_1 \supset F_2 \supset \cdots \supset F_n = F$. By the definition of conditional probability, the failure probability of the pipeline can be expressed as a product of conditional probabilities,

$$P(F) = P(F_1)\prod_{i=1}^{n-1} P(F_{i+1}|F_i) = \prod_{i=1}^{n} P_i \tag{31}$$

where $P_1$ denotes $P(F_1)$ and $P_i(i = 2,3,\cdots,n)$ denotes $P(F_i|F_{i-1})$. Eq. (32) expresses a small failure probability as a product of relatively large conditional probabilities. For example, assume $P_i \sim 0.1, i = 1,2,\cdots 4$, then the failure probability $P(F) \sim 10^{-4}$ which is too small for efficient estimation by MCS. However, the conditional probabilities $P_i(i = 1,2,\cdots 4)$, are of order $0.1$, and so can be evaluated efficiently by simulation.

The probability $P_1$ can be evaluated readily by the application of direct MCS simulation as

$$P_1 = \frac{1}{N_1}\sum_{h=1}^{N_1} I_{F_1}\left(\boldsymbol{\theta}_h^{(1)}\right) \tag{32}$$

400 in which $\boldsymbol{\theta}_h^{(1)}(h = 1,2,\cdots,N_1)$ are independently distributed samples simulated from
401 the PDF $q(\boldsymbol{\theta})$, and $N_1$ is the number of samples $\boldsymbol{\theta}_h^{(1)}$.

402 To estimate the conditional probabilities $P_i(i = 2,3,\cdots,n)$ samples should be
403 generated according to the conditional PDF $q(\boldsymbol{\theta}|F_{i-1}) = q(\boldsymbol{\theta})I_{F_i}(\boldsymbol{\theta})/P(F_{i-1})$. However,
404 efficient sampling from a conditional PDF is usually not a trivial task. Fortunately, this
405 can be achieved by the Markov chain Monte Carlo (MCMC) simulation based on the
406 Metropolis-Hastings (M-H) algorithm which provides a powerful method for generating
407 samples that satisfy the prescribed conditional probability. Readers are referred to [23]
408 for more details regarding the MCMC and the modified M-H algorithm.

409 After generating the conditional samples, the conditional failure probability $P_i$ can
410 be determined as
411

$$P_i = \frac{1}{N_i}\sum_{h=1}^{N_i} I_{F_i}\left(\boldsymbol{\theta}_h^{(i)}\right) \tag{33}$$

412
413 where $\boldsymbol{\theta}_h^{(i)}(h = 1,2,\cdots,N_i)$ are independent distributed conditional samples according
414 to the conditional density probability $q(\boldsymbol{\theta}|F_{i-1})$. Through choosing the intermediate
415 threshold values $b_i$ adaptively, the conditional probabilities $P_i(i = 1,2,\cdots,n-1)$ can
416 be ensured to be equal to a certain value $p_0$ ($p_0 = 0.1$ is used here). Substituting Eqs.
417 (32) and (33) into Eq. (31), the failure probability can be expressed as
418

$$P_F = p_0^{n-1}\frac{1}{N_n}\sum_{h=1}^{N_n} I_{F_n}\left(\boldsymbol{\theta}_h^{(n)}\right) \tag{34}$$

419

420 The main procedures of SS can be summarized as follows.

421 1. Generate $N$ samples $\boldsymbol{\theta}_h^{(0)}(h = 1,2,\cdots,N)$ by direct MCS from the original PDF

422 $q(\boldsymbol{\theta})$. The superscript "0" denotes these samples correspond to conditional level 0.

423 2. Set $i = 0$.

424 3. Calculate the corresponding response variable $\tilde{\boldsymbol{s}}\left(\boldsymbol{\theta}_h^{(i)}\right) = \max\left(\left|\boldsymbol{s}\left(t, \boldsymbol{\theta}_h^{(i)}\right)\right|\right)$

425 4. Choose the intermediate threshold value $b_{i+1}$ as the $(1 - p_0)N$th value in the

426 ascending order of $\tilde{\boldsymbol{s}}\left(\boldsymbol{\theta}_h^{(i)}\right)$ (calculated at step 3). Hence the sample estimate of $P_{i+1}$ is

427 always equal to $p_0$. Note that it has been assumed that $p_0 N$ is an integer value.

428 5. If $b_{i+1} > b_n$, proceed to step 10 below.

429 6. Otherwise, if $b_{i+1} < b$, with the choice of $b_{i+1}$ performed at step 4, identify the

430 $p_0 N$ samples $\boldsymbol{\theta}_H^{(i)}(H = 1,2,\cdots,p_0 N)$ among $\boldsymbol{\theta}_h^{(i)}(h = 1,2,\cdots,N)$ whose response

431 $\tilde{\boldsymbol{s}}\left(\boldsymbol{\theta}_H^{(i)}\right)$ lies in the region $F_{i+1} = \left\{\tilde{\boldsymbol{s}}\left(\boldsymbol{\theta}_H^{(i)}\right) > b_{i+1}\right\}$. These samples are at conditional

432 level $i + 1$ and distributed as the conditional probability $q(\quad|F_{i+1})$.

433 7. The samples $\boldsymbol{\theta}_H^{(i)}(H = 1,2,\cdots,p_0 N)$ (identified at step 6) provide seeds for

434 applying the MCMC simulation to generate $(1 - p_0)N$ additional conditional samples

435 distributed as the conditional probability $q(\quad|F_{i+1})$, so that it obtains a total of $N$

436 conditional samples $\boldsymbol{\theta}_h^{(i+1)}(h = 1,2,\cdots,N) \in F_{i+1}$ at conditional level $i + 1$.

437 8. Set $i \leftarrow i + 1$.

438 9. Return to step 3 above.

439 10. Stop the algorithm.

It is noted that the total number of samples employed is $N_T = N + (n-1)(1-p_0)N$.

The sensitivity of the reliability with respect to variations in system parameters reflects the contributions of these parameters to the failure of structures, and hence it is useful to perform a reliability sensitivity analysis. The reliability sensitivity is defined as the partial derivative of the failure probability with respect to distributional parameters of the system parameter. In the framework of SS, the reliability sensitivity can be expressed as [36]

$$\left.\frac{\partial P_F}{\partial \eta}\right|_{\bar{\eta}} = p_0^{n-1}\frac{1}{N_n}\sum_{h=1}^{N_n} I_{F_n}\left(\boldsymbol{\theta}_h^{(n)}\right)\frac{\dfrac{\partial q\left(\boldsymbol{\theta}_h^{(n)}\right)}{\partial \eta}}{q\left(\boldsymbol{\theta}_h^{(n)}\right)} \tag{35}$$

where $\eta$ denotes the distribution parameters, for example, the mean value or the standard deviation, of the PDF of the uncertain system parameters $\boldsymbol{\theta}$. $\bar{\eta}$ is the value of the distribution parameter where the sensitivity is evaluated. For a better comparison of the contribution of different system parameters, the reliability sensitivity can be normalized as follows,

$$e_\eta = \frac{\partial P_F}{\partial \eta}\frac{\bar{\eta}}{P_F} \tag{36}$$

# 5 Numerical examples

In the following numerical examples, information about the system parameters is

given first. Then, SS is applied for estimating the failure probability of a subsea pipeline subjected to a random earthquake with spatial variation, and a comparison is made with the direct MCS (DMCS) to verify the SS. Then a sensitivity and failure analysis is performed to identify the influential parameters on the pipeline failure. Finally, the reliabilities of subsea pipelines in three typical cases are investigated.

## 5.1 Description of system parameters

The subsea pipeline in Fig. 1 is adopted as an example structure. Unless otherwise specified, the physical and geometric parameters of the pipeline are as follows: material grade X60 with specified minimum yield strength (SMYS) $\sigma_y = 414 \times 10^6$Pa, Young's modulus $E = 207 \times 10^9$Pa, mass density $\rho_{\text{pipe}} = 7850\,\text{kg/m}^3$, Poisson's ratio $\nu = 0.3$, Rayleigh damping factors corresponding to the mass $d_1 = 0.01$ and the stiffness $d_2 = 0.05$, total length of pipeline $L_0 = 100\text{m}$, shear correction factor $\kappa = 2(1+\nu)/(4+3\nu)$, outer radius $R_{\text{out}} = 0.6\text{m}$, wall thickness $h = 0.02\text{m}$. The mass densities of the oil in the pipeline and surrounding water are $\rho_{\text{oil}} = 800\,\text{kg/m}^3$ and $\rho_{\text{water}} = 1025\,\text{kg/m}$, respectively, and the velocity of the oil is $3\,\text{m/s}$. According to the design standard [4], the effective axial compression $N_0$ should not exceed $0.5N_{\text{cr}}$, where $N_{\text{cr}}$ is the critical buckling load, and hence $N_0 = 0.3N_{\text{cr}}$ is used in this paper. The pipeline is discretized into 100 elements and both ends are simply supported. The failure criterion for the subsea pipeline is defined as when the bending stress exceeds 80% of SMYS [37].

The location and length of the free span, $L_1$ and $L_2$, are assumed to be Gaussian distributed variables with mean values $50\text{m}$ and $30\text{m}$, respectively, and coefficient of variation (COV) 0.3. As physical parameters these must be strictly positive, and in order to guarantee that one free span always exists, $L_1$ and $L_2$ are required to satisfy the following constraints,

$$\begin{cases} L_0 \geq L_2 \geq 0 \\ L_1 - L_2/2 \geq 0 \\ L_0 - L_1 - L_2/2 \geq 0 \end{cases} \tag{37}$$

Strictly speaking, these constraints rule out the use of Gaussian models for the random variables $L_1$ and $L_2$. Hence, an acceptance-rejection method is used to generate samples of $L_1$ and $L_2$ from Gaussian distributions with constraints as expressed in Eq. (37).

The maximum depth of the free span $h_{\text{free}} = 0.3\text{m}$ and the stiffness of the seabed $k_{\text{seabed}} = 2.293 \times 10^6\ \text{N/m}^2$ are used here. Parameters of the ground motion PSD and the spatial variation are respectively $S_{\text{g}} = 0.018\,\text{m}^2/\text{s}^3$, $\omega_{\text{g}} = 15\,\text{rad/s}$, $\omega_{\text{f}} = 0.1\omega_{\text{g}}$, $v_{\text{app}} = 1000\,\text{m/s}$, $\xi_{\text{g}} = \xi_{\text{f}} = 0.6$ [38]. The duration of the earthquake is $T = 10.92\text{s}$, and the time step for the numerical integration is $\Delta t = 0.01\text{s}$. Hence the number of time steps is $N_t = 1093$. In order to generate the ground motion time histories from the above ground PSD, the following procedures are implemented. A $N_{\text{node}} \times N_t$ discrete-time white noise matrix $\boldsymbol{W}$ is first generated, where the elements of $\boldsymbol{W}$ have a mean value of 0 and standard deviation of $\sqrt{2\pi/\Delta t}$, $N_{\text{node}}$ is the number of nodes of the discrete pipeline. Then the ARMA method is used to modulate $\boldsymbol{W}$ to generate the required

499 ground motion samples.

500 During the SS procedures, the choice of the proposal PDF and the grouping of
501 uncertain parameters affect the distribution and the acceptance rate of the samples and
502 consequently the efficiency of the SS. It is suggested in [29] that deciding what type of
503 proposal PDF to use for a group depends on the contribution of the uncertain parameters
504 to the failure and on the information available for constructing the proposal PDF. In this
505 paper, there are two types of uncertain parameters. The first type is the discrete-time white
506 noise matrix $\boldsymbol{W}$, whose parameters play a similar role in affecting failure. These
507 parameters affect failure significantly as a whole, but not individually. Hence, each of
508 these parameters is grouped individually and their proposal PDFs can be chosen to be
509 uniform with width 2. The second type is the structural parameters $L_1$ and $L_2$, whose
510 contribution to the failure cannot be known a priori. Hence, $L_1$ and $L_2$ are collected
511 into one group and the proposal PDF is chosen to be Gaussian with mean and covariance
512 estimated from the current seed samples.

513 ## 5.2 Validation of the subset simulation

514 SS and DMCS are used to estimate the failure probability of the subsea pipeline
515 under the earthquake and the results are shown in Fig. 2. SS is applied with a conditional
516 failure probability $p_0 = 0.1$ and the number of samples at each level is $N = 1000$. Four
517 levels of conditional simulations are used in one simulation run, so the total number of
518 samples is $N_T = 3700$. For comparison, the failure probabilities from the DMCS with

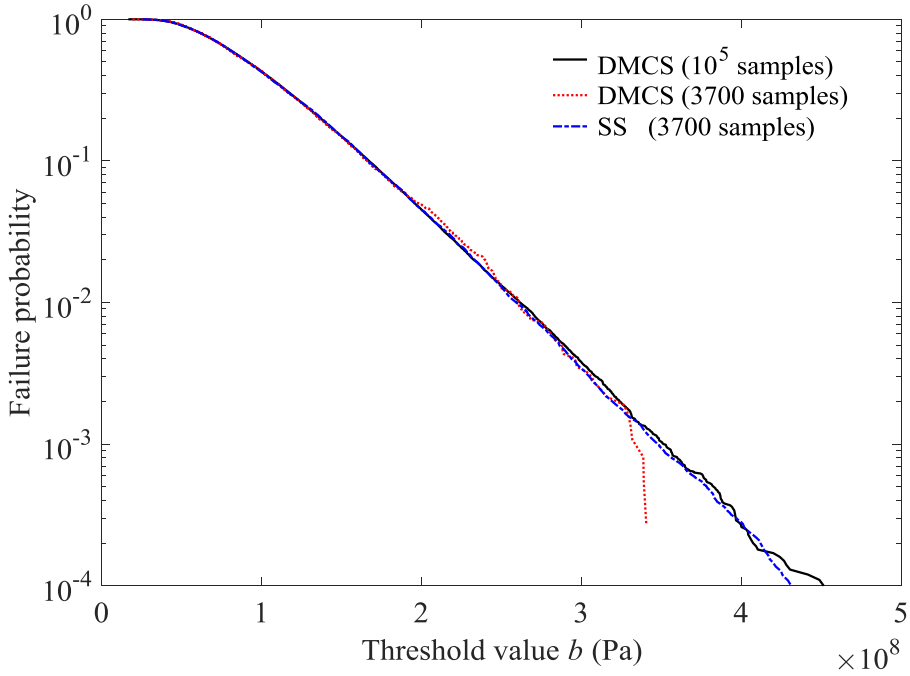


519

520 **Fig. 2.** Comparison of failure probability from SS and DMCS

521

522 $10^5$ and 3700 samples are also given in Fig. 2. It is seen that the results of these three
523 simulation cases agree very well in the region with relative large failure probability
524 (above $10^{-2}$). However, in the region with small failure probability (below $10^{-3}$),
525 results of SS and DMCS with $10^5$ samples still agree quite well, while those of the
526 DMCS with 3700 samples show a significant discrepancy.

527 To investigate the variability of the SS results, the COV of the failure probability
528 from 10 independent SS runs is shown in Fig. 3. Since each conditional level contains
529 1000 samples, the total numbers of samples, $N_T$, used for obtaining estimates of failure
530 probability level at $10^{-1}$, $10^{-2}$, $10^{-3}$ and $10^{-4}$ are 1000, 1900, 2800 and 3700,
531 respectively. For comparison, the COV of the results of the DMCS are given at particular

failure probability level by using the same total numbers of samples. It should be noted that DMCS is unable to estimate the failure probability accurately with a relatively small number of samples, e.g., 3700, so the COV of DMCS is obtained from an simple approximate formula [23], i.e., $\mathrm{COV} = \sqrt{\big(1 - P(F)\big)/(P(F)N)}$, rather than from many independent DMCS runs. It can be seen from Fig. 3 that the COV of SS increases gradually with decreasing failure probability, while the COV of DMCS increases much more rapidly. The COV of SS and DMCS are quite close in the region with relatively large failure probability ($10^{-2}$~$10^{-1}$). However, when the failure probability is below $10^{-3}$, it can be observed that the COV of DMCS is much larger than that of SS.

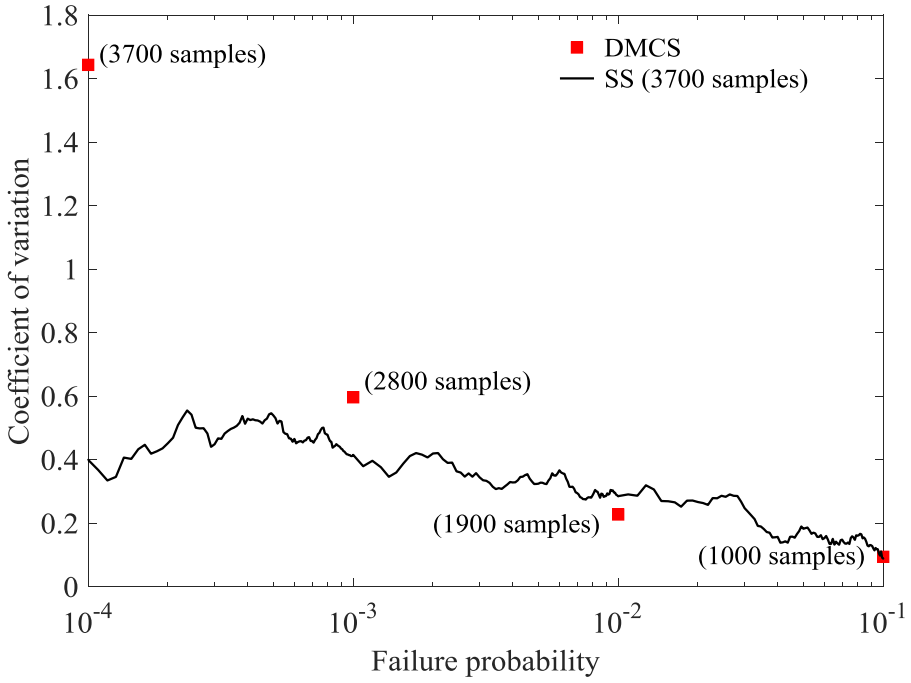


**Fig. 3.** Comparison of the COV of the failure probabilities from SS and DMCS

The results in Fig. 2 and 3 show that, compared to DMCS, SS can estimate the failure probability with much fewer samples, and its results have a smaller COV, especially in the low failure probability region. Hence, SS is proved to be a highly accurate and robust method to estimate the small failure probability of subsea pipelines under a random earthquake.

## 5.3 Sensitivity and failure analysis

To identify the contribution of the uncertain structural parameters to the failure of the subsea pipeline, a sensitivity analysis of the failure probability with respect to the mean values and variations of $L_1$ and $L_2$ is performed using SS, and the results are compared to those of DMCS, as shown in Table 1. It can be observed that the results of SS and DMCS agree quite well from the perspective of the sensitivity which is in fact a higher order quantity. It is also observed that the sensitivity with respect to $L_2$ is larger than that with respect to $L_1$, implying that the length of the free span $L_2$ is more influential on the failure of subsea pipelines than its location $L_1$.

The Markov chain samples generated during SS can be used not only for estimating the conditional probabilities, but also for the failure probability [29]. From Bayes' theorem,

$$P(F|\boldsymbol{\theta}_l) = \frac{q(\boldsymbol{\theta}_l|F)}{q(\boldsymbol{\theta}_l)} P(F), \qquad l = 1,2 \cdots N_{\boldsymbol{\theta}} \tag{39}$$

565 **Table 1** Normalized sensitivities of the failure probability

| | SS | DMCS |
|---|---|---|
| $e_{\mu_{L_1}}$ | 0.147 | 0.125 |
| $e_{\mu_{L_2}}$ | 1.035 | 0.893 |
| $e_{\sigma_{L_1}}$ | 0.0371 | 0.0439 |
| $e_{\sigma_{L_1}}$ | 0.348 | 0.298 |

566

567 where $N_{\boldsymbol{\theta}}$ is the dimension of $\boldsymbol{\theta}$. Thus when $q(\boldsymbol{\theta}_l|F)$ is similar to $q(\boldsymbol{\theta}_l)$, it is deduced
568 that $P(F|\boldsymbol{\theta}_l) \approx P(F)$, so that the failure probability is insensitive to $\boldsymbol{\theta}_l$. Hence, by
569 comparing the conditional PDF $q(\boldsymbol{\theta}_l|F)$ with the unconditional PDF $q(\boldsymbol{\theta}_l)$, one can
570 obtain an indication of how much the uncertain parameter $\boldsymbol{\theta}_l$ influences the system
571 failure.

572 Fig. 4 shows histograms of the conditional samples of the uncertain parameters $L_1$
573 and $L_2$ at different levels for a single SS run. It is noticed that the conditional PDFs of
574 the uncertain parameters are obviously too large for certain values. This is because there
575 are inevitably some repeated samples during the MCMC procedure. Despite some peaks,
576 it is seen that the conditional PDFs of $L_1$ are almost symmetric about the mean value of
577 $L_1$ at different levels, while those of $L_2$ are not symmetric and have a significant
578 rightward shift, especially at the final level. From the comparison of the shapes of the
579 conditional PDFs, it is concluded qualitatively that $L_2$ contributes more to the failure

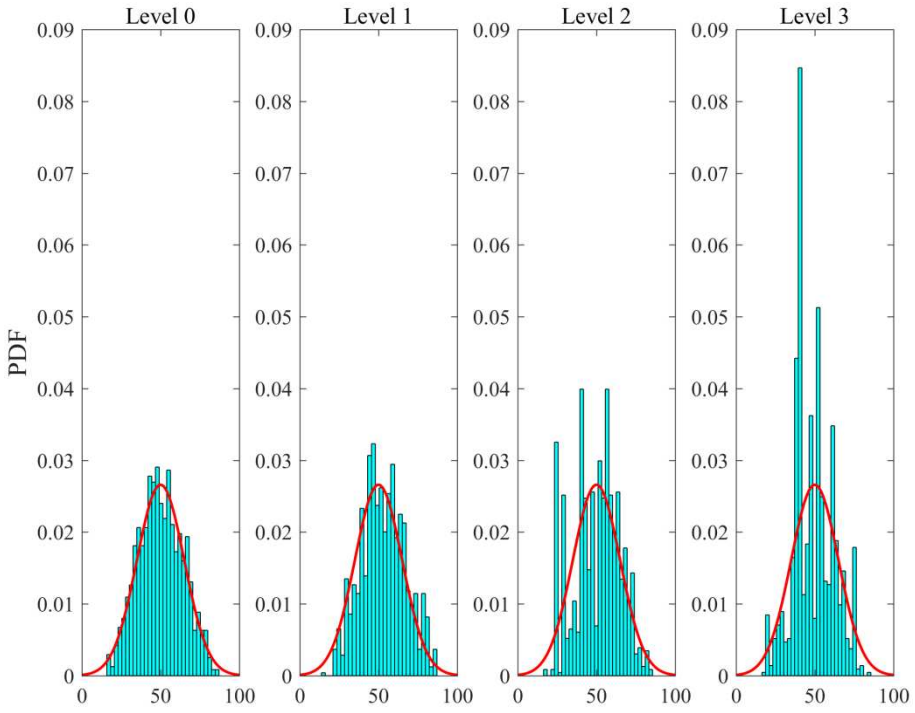


(a) $L_1$

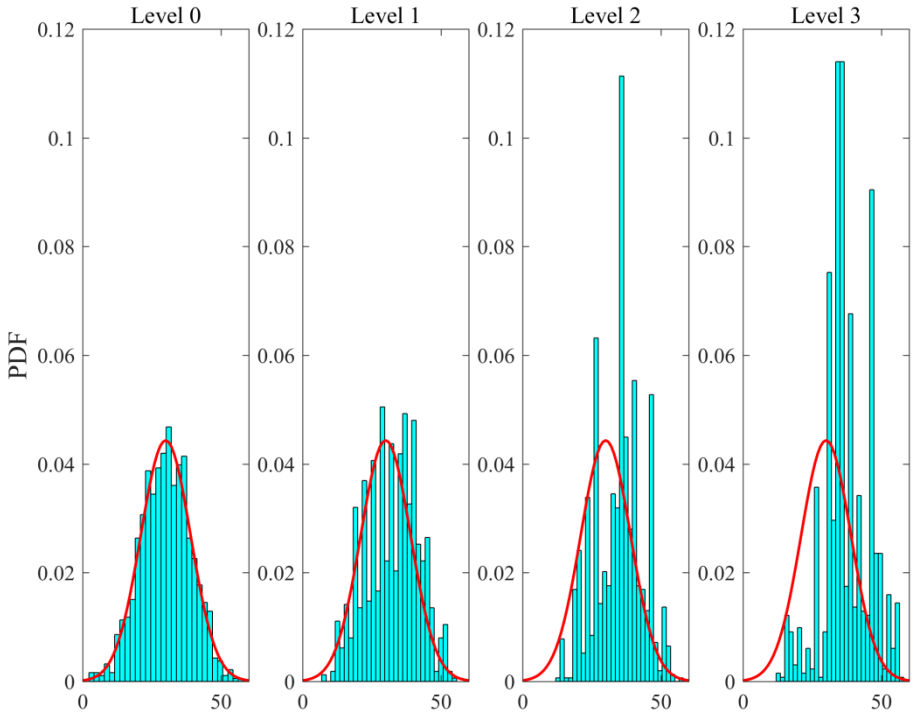


(b) $L_2$

**Fig. 4.** Empirical conditional PDFs of $L_1$ and $L_2$ at different conditional levels (histograms) compared to their unconditional PDFs (solid lines)

of subsea pipelines than L_1. This is in agreement with the conclusion of the parametric sensitivity analysis above.

## 5.4 Study of three typical cases

To study the influences of more parameters or effects on the failure of subsea pipelines, three typical cases are considered.

**Case 1:** *Unilateral contact model and permanent contact model*

As pointed out in the introduction, the separation of pipelines and the seabed is not considered in the dynamic analysis in some literature [5, 6]. This pipeline-seabed model is called a “permanent contact model”, while the model used in this paper is called a “unilateral contact model”. In order to investigate the influence of the unilateral contact effect on the reliability of subsea pipelines, failure probabilities of the unilateral and permanent models are calculated by SS and results are shown and compared in Fig. 5. It is seen that the failure probability of the permanent contact model is smaller than that of the unilateral contact model at the same threshold value, so that the permanent contact model is a more dangerous model in the earthquake design of subsea pipelines. The comparison also shows the necessity of the consideration of the unilateral contact effect in the earthquake reliability analysis of subsea pipelines.

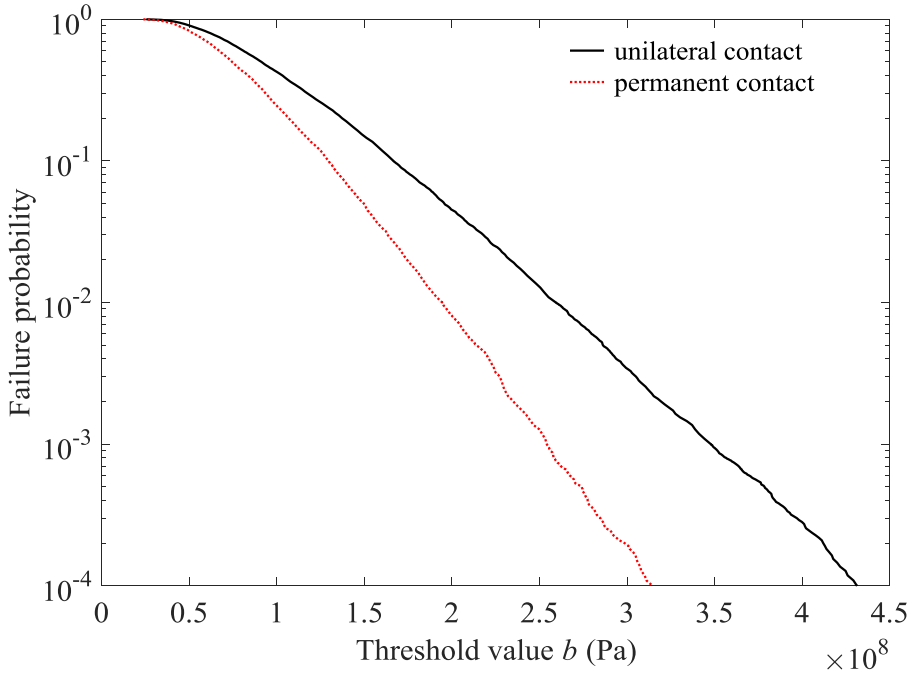


603

604 **Fig. 5.** Failure probabilities of subsea pipelines using unilateral and permanent contact

605 models

606 **Case 2**: *Different apparent velocity*

607 As expressed in Eqs. (12) and (13), the apparent velocity of the earthquake waves $v_{\text{app}}$

608 is one of the most important parameters affecting the spatial variation of the ground

609 motion. The spatial variation decreases with increasing $v_{\text{app}}$. When $v_{\text{app}}$ approaches

610 infinity, the spatial variation of the ground motion vanishes and the earthquake is reduced

611 to a uniform excitation. To study the influences of the spatial variation of the ground

612 motion on the reliability, four cases with different $v_{\text{app}}$ are considered, namely $v_{\text{app}} =$

613 $500\,\text{m/s}$, $1000\,\text{m/s}$, $2000\,\text{m/s}$ and uniform excitation, as shown in Fig. 6. It is

614 observed that the influence of $v_{\text{app}}$ on failure is not significant in the region with relative

615 large failure probability. But when the failure probability is at a small level, it increases

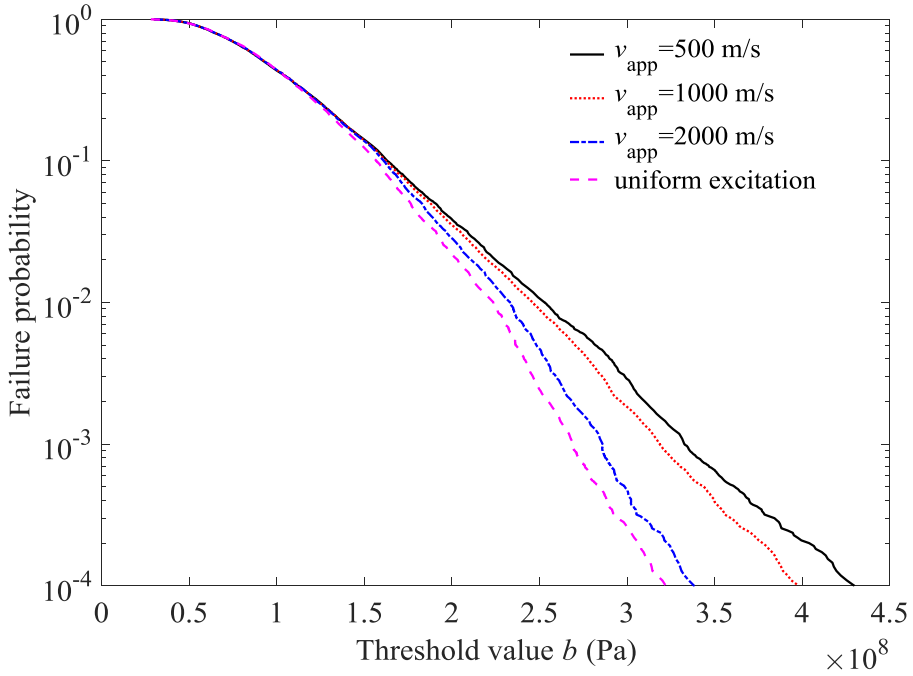


616

617 **Fig. 6.** Failure probabilities of subsea pipeline with different apparent velocity $v_{\text{app}}$

618

619 with decreasing apparent velocity $v_{\text{app}}$.

620 **Case 3**: *With and without free span*

621 In subsection 5.3, sensitivities of the failure probability of pipelines with respect to the
622 location and length of the free span were studied. To study further the influence of the
623 free span itself on the failure of subsea pipelines, three different cases are considered, i.e.,
624 (1) without free span, (2) with a deterministic free span at location $L_1 = 50\text{m}$ with
625 length $L_2 = 30\text{m}$ and (3) with the uncertain free span used in subsection 5.3. The results
626 are given in Fig. 7. It is shown that the free span has significant influence on the reliability
627 of the subsea pipeline. Neglect of the free span or its uncertainty in the earthquake
628 reliability analysis will lead to an underestimate of the failure probability.

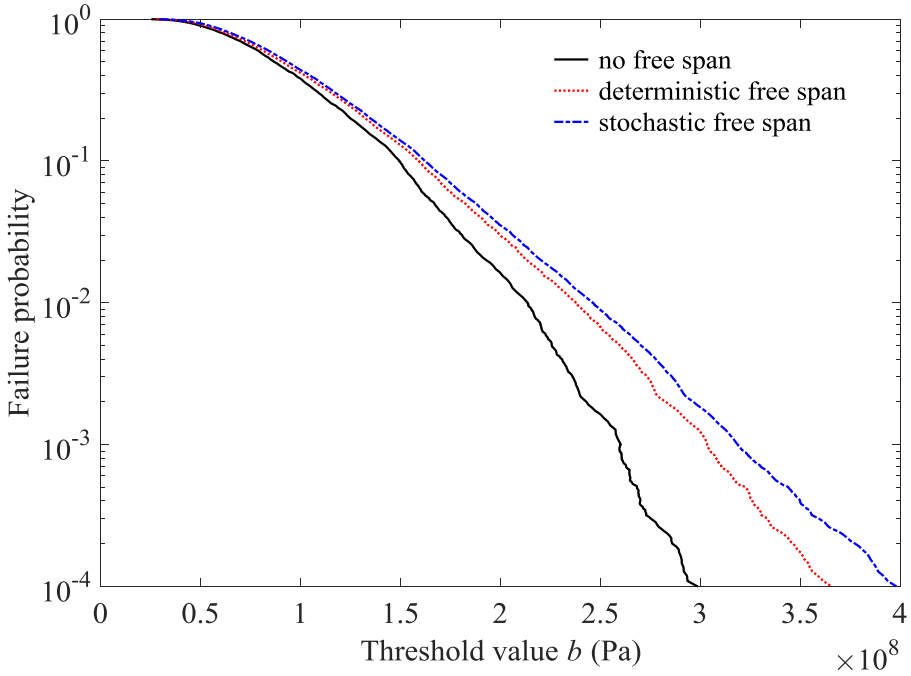


**Fig. 7.** Failure probabilities of subsea pipeline with different types of free span

# 6 Conclusions

In this paper, a computational framework based on subset simulation (SS) is proposed for the reliability analysis of subsea pipelines subjected to a random earthquake with spatial variation. Firstly, a mathematical model of subsea pipelines under random earthquake is established with consideration of the unilateral contact effect between the pipeline and the seabed. Then, by using the finite element method and Newmark integration method, the governing equation is discretized and the dynamic contact problem is derived as a linear complementarity problem. Finally, SS is applied for estimating the failure probability of subsea pipelines. SS expresses a small failure probability as a product of a sequence of large conditional probabilities, and provides the

potential to reduce the number of samples required in estimating small failure probability.

In numerical examples, direct Monte Carlo simulation (DMCS) is used to validate the feasibility of SS in the earthquake reliability problem. It is found that the failure probabilities calculated by SS agree well with those from DMCS, while the efficiency of SS, as indicated by the smaller number of samples, is much greater than that of DMCS. A coefficient of variation analysis shows that SS is more robust in small failure probability estimation than DMCS. Results from a sensitivity analysis indicate that the free span length is more influential on the failure of subsea pipelines than the free span location. Three typical cases with different parameters or effects are studied. It is shown that the unilateral contact effect between the seabed and pipelines, the spatial variation of the ground motion and the uncertainty of the free span have great influence on the failure of seabed pipelines and should be considered in earthquake reliability analysis.

## Acknowledgments

The authors are grateful for support under grants from the National Basic Research Program of China (2014CB046803), the National Science Foundation of China (11672060), and the Cardiff University Advanced Chinese Engineering Centre.

# References


[1] Teixeira AP, Guedes Soares C, Netto TA, Estefen SF. Reliability of pipelines with corrosion defects. Int J Press Vessels Pip 2008; 85(4): 228-237.

[2] Elosta H, Huang S, Incecik A. Wave loading fatigue reliability and uncertainty analyses for geotechnical pipeline models. Ships Offshore Struct 2014; 9(4): 450-463.

[3] Elsayed T, Leheta H, Yehya A. Reliability of subsea pipelines against lateral instability. Ships Offshore Struct 2012; 7(2): 229-236.

[4] Det Norsk Veritas. Submarine Pipeline Systems. DNV-OS-F101, 2007.

[5] Lin YK, Zhang R, Yong Y. Multiply supported pipeline under seismic wave excitations. J Eng Mech 1990; 116(5): 1094-1108.

[6] Soliman HO, Datta TK. Response of overground pipelines to random ground motion. Eng Struct 1996; 18(7): 537-545.

[7] Xu T, Lauridsen B, Bai Y. Wave-induced fatigue of multi-span pipelines. Mar Struct 1999; 12(2): 83-106.

[8] Sollund HA, Vedeld K, Fyrileiv O. Modal response of short pipeline spans on partial elastic foundations. Ocean Eng 2015; 105: 217-230.

[9] Maier G, Andreuzzi F, Giannessi F, Jurina L, Taddei F. Unilateral contact, elastoplasticity and complementarity with reference to offshore pipeline design. Comput Methods Appl Mech Eng 1979; 17-18: 469-495.

681 [10] Kalliontzis C, Andrianis E, Spyropoulos K, Doikas S. Finite element stress analysis
682 of unilaterally supported submarine pipelines. Comput Struct 1996; 61(6): 1207-
683 1226.
684 [11] Baniotopoulos CC. Optimal control of submarine cables in unilateral contact with
685 the sea-bed profile. Comput Struct 1989; 33(2): 601-608.
686 [12] Panagiotopoulos P D. Inequality Problems in Mechanics and Applications: Convex
687 and Nonconvex Energy Functions. Birkhauser, Boston, 1985.
688 [13] Der Kiureghian A. A coherency model for spatially varying ground motions. Earthq
689 Eng Struct Dyn 1996; 25(1): 99-111.
690 [14] Lin J H. A fast CQC algorithm of PSD matrices for random seismic responses.
691 Comput Struct 1992; 44(3): 683-687.
692 [15] Der Kiureghian A, Neuenhofer A. Response spectrum method for multi-support
693 seismic excitations. Earthq Eng Struct Dyn 1992; 21(8): 713-740.
694 [16] Heredia-Zavoni E, Vanmarcke EH. Seismic random-vibration analysis of
695 multisupport-structural systems. J Eng Mech 1994; 120(5): 1107-1128.
696 [17] Shinozuka M. Monte Carlo solution of structural dynamics. Comput Struct 1972;
697 2(5-6): 855-874.
698 [18] Hohenbichler M, Rackwitz R. First-order concepts in system reliability. Struct Saf
699 1982; 1(3): 177-188.
700 [19] Der Kiureghian A, Lin HZ, Hwang SJ. Second-order reliability approximations. J

Eng Mech 1987; 113(8): 1208-1225.

[20] Hong HP. An efficient point estimate method for probabilistic analysis. Reliab Eng Syst Saf 1998; 59(3): 261-267.

[21] Melchers RE. Importance sampling in structural systems. Struct Saf 1989; 6(1): 3-10.

[22] Engelund S, Rackwitz R. A benchmark study on importance sampling techniques in structural reliability. Struct Saf 1993; 12(4): 255-276.

[23] Au SK, Beck JL. Estimation of small failure probabilities in high dimensions by subset simulation. Probabilist Eng Mech 2001; 16(4): 263-277.

[24] Au SK, Ching J, Beck JL. Application of subset simulation methods to reliability benchmark problems. Struct Saf 2007; 29(3): 183-193.

[25] Tee KF, Khan LR, Li HS. Application of subset simulation in reliability estimation of underground pipelines. Reliab Eng Syst Saf 2014; 130: 125-131.

[26] Yuan J, Allegri G, Scarpa F, Rajasekaran R, Patsias S. Probabilistic dynamics of mistuned bladed disc systems using Subset Simulation. J Sound Vib 2015; 350: 185-198.

[27] Cadini F, Avram D, Pedroni N, Zio E. Subset Simulation of a reliability model for radioactive waste repository performance assessment. Reliab Eng Syst Saf 2012; 100: 75-83.

[28] Vahdatirad MJ, Andersen LV, Ibsen LB, Sørensen JD. Stochastic dynamic stiffness

721 of a surface footing for offshore wind turbines: Implementing a subset simulation
722 method to estimate rare events. Soil Dyn Earthq Eng 2014; 65: 89-101.
723 [29] Au SK, Beck JL. Subset simulation and its application to probabilistic seismic
724 performance assessment. J Eng Mech 2003; 129(8): 901-917.
725 [30] Paidoussis MP, Laithier BE. Dynamics of Timoshenko beams conveying fluid. J
726 Mech Eng Sci 1976; 18(4): 210-220.
727 [31] Morison JR, Johnson JW, Schaaf SA. The force exerted by surface waves on piles. J
728 Petrol Technol 1950; 2(5): 149-154.
729 [32] Loh CH, Yeh YT. Spatial variation and stochastic modelling of seismic differential
730 ground movement. Earthq Eng and Struct Dyn 1988; 16(4): 583-596.
731 [33] Clough R W, Penzien J. Dynamics of Structures. New York: McGraw-Hill, 1993.
732 [34] Samaras E, Shinzuka M, Tsurui A. ARMA representation of random processes. J Eng
733 Mech 1985; 111(3): 449-461.
734 [35] Berg GV, Housner GW. Integrated velocity and displacement of strong earthquake
735 ground motion. B Seismol Soc Am 1961; 51(2): 175-189.
736 [36] Jensen HA, Mayorga F, Valdebenito MA. Reliability sensitivity estimation of
737 nonlinear structural systems under stochastic excitation: A simulation-based
738 approach. Comput Methods Appl Mech Eng 2015; 289: 1-23.
739 [37] Arifin RB, Yusof WM, Zhao PF, Bai Y. Seismic analysis for the subsea pipeline
740 system. In: Proceedings of the ASME 2010 29th International Conference on Ocean,

741 Offshore and Arctic Engineering, OMAE2010-20671, Shanghai, China, 2010.

742 [38] Dumanogluid AA, Soyluk K. A stochastic analysis of long span structures subjected

743 to spatially varying ground motions including the site-response effect. Eng Struct

744 2003; 25(10): 1301-1310.